A Study of an Inversion Model for Sea Ice Thickness Retrieval Using Simulated Annealing

Yu Jen Lee*, Kee Choon Yeong, and Hong Tat Ewe

Abstract—Previously, an inverse microwave scattering model based on radiative transfer was developed for the retrieval of sea ice thickness using radar backscatter data. The model, called the Radiative Transfer Inverse Scattering Model (RTISM), is a combination of the Radiative Transfer-Dense Medium Phase and Amplitude Correction Theory (RT-DMPACT) forward model and the Levenberg-Marquardt Algorithm (LMA). In this paper, the LMA in the RTISM is replaced with Simulated Annealing (SA) as the optimizer to allow a wider range of inversion capability. SA is a global optimizer, and its settings make it convenient to switch between different target parameters to be optimized for inversion. In this study, the model will first be tested using different data sets to verify its applicability. Next, the model is used to estimate the sea ice thickness around Ross Island, Antarctica using data from ground truth measurements together with satellite data from Radarsat-1 from the year 2006. In order to further validate the model, the data collected from measurements performed during an experiment to grow an ice sheet within a refrigerated facility at the U.S. Army Cold Regions Research and Engineering Laboratory (CRREL) are used to perform the retrieval of saline ice thickness. Preliminary results show that the new model performs as expected and shows potential. However, there are still limitations to the inverse model, and further improvements in the future need to be considered.

1. INTRODUCTION

Ever since the first explorers began expeditions to the polar region, both the Arctic and Antarctica have intrigued generations of adventurers, scientists, and researchers. Since then, studies in polar physical science and biological science have rapidly grown and expanded, greatly enhancing the understanding of these extreme locations on Earth. The onset of climate change has further intensified the interest in these regions. Studies have shown that changes in the polar region are strong indicators of global warming [1]. The collapse of the Larsen B Ice Shelf back in 2002 and the recession of glaciers are but a few examples of climate change [2, 3]. Recent research has further shown a decline in global sea ice extent, especially in the Arctic [4]. With the changing of the world climate in the past few decades, the interest in the sea ice and ice shelves found in the polar region has increased dramatically.

The collapse of ice shelves, recession of glaciers, and the reduction of sea ice extent are worrying mainly because the formation and melting of the sea ice modulate the heat and moisture exchange between the atmosphere and ocean and also control the flow of the current in the world's oceans [5]. This in turn affects the complex interactions of the ecosystem and sea water levels. Many studies have been carried out in a bid to better understand how climate change affects the polar region and how these changes in return impact the tropics. Such studies usually require huge amounts of physical data, which can be difficult to obtain via ground truth measurements due to the harsh environment of the polar region.

The development and advancement of airborne and spaceborne remote sensing technology using synthetic aperture radar (SAR) installed on drones, aircraft or satellite, to carry out wide area monitoring without the need of human presence offers a possible solution. After the remote sensing data is collected, another challenge is the interpretation of the data for the use of various remote sensing applications. This is where theoretical models can come in and assist. While forward models, such as those reported in [6], allow the comprehension of the scattering mechanisms by the different properties of sea ice, inverse scattering models are required to process the remote sensing data into physical parameters of sea ice. In [7], it is highlighted that one of the important parameters in the study of climate change is the sea ice thickness.

Previously, an inverse scattering model for the retrieval of sea ice thickness was proposed [8]. The inverse model, named the Radiative Transfer Inverse Scattering Model (RTISM), was loosely based on the time-series inverse scattering model developed by Shih et al. [9, 10]. In the RTISM, the ice growth model in [9, 10] was not used as it requires extensive measurement data and satellite data during the growing stages of the sea ice. The authors instead focused on first year sea ice and performed a multiyear analysis of all the parameters collected from ground truth measurements from 2002–2008 and used the statistics of these parameters to perform the inversion. Additionally, a sensitivity analysis was also performed to observe the sensitivity of the forward model to variations in the sea ice thickness.

While the model itself functions properly, the inverse model becomes ineffective in cases where the sea ice is very thick ($\sim 1.7\,\text{m}$), and radar backscatter saturates. Lastly, the authors noted that the extension of the model to retrieve other parameters can be tedious, as the use of the Levenberg Marquadt Algorithm (LMA) requires the calculation of Jacobian matrices of the problem function with respect to the target parameter. With these shortcomings in mind, there is a need to improve the RTISM. This modification will be discussed in the next section.

2. RADIATIVE TRANSFER INVERSE SCATTERING MODEL (RTISM) WITH SIMULATED ANNEALING (SA)

In this paper, the RTISM is modified by replacing the LMA with a different optimizer, Simulated Annealing (SA) [11] and will be called RTISM-SA. While the LMA is robust and performs well in most optimization cases, it is a local optimizer, thus risking being trapped in the local optima. Additionally,
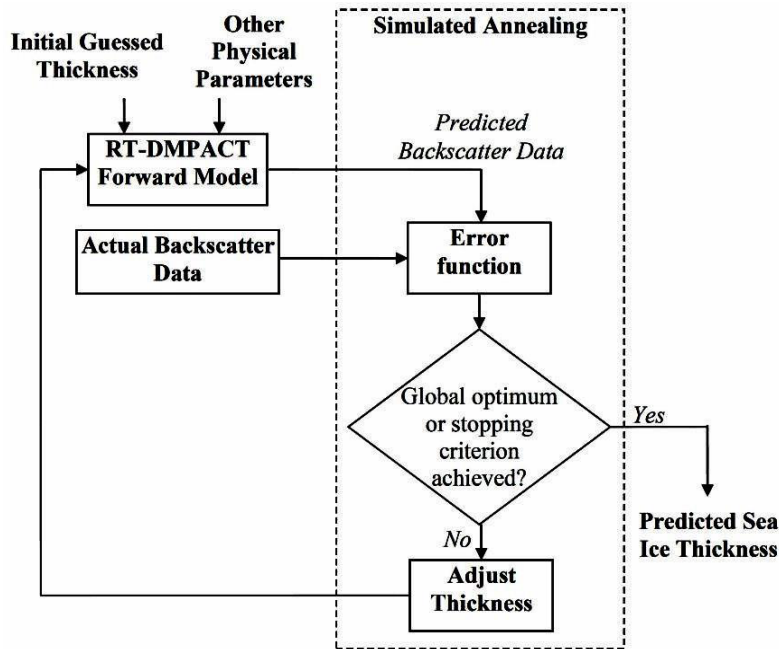

Figure 1. Flowchart for RTISM with simulated annealing.

it also requires the calculation of the Jacobian matrices of the problem function with respect to the target parameter. The main aim of the study is to modify the RTISM so that it can be easily changed to retrieve parameters other than sea ice thickness and also to improve the convergence rate. The authors found SA to be suitable as a replacement for this purpose. A detailed flowchart of RTISM-SA for Sea Ice Thickness Retrieval is shown in Figure 1.

From Figure 1, a set of physical parameters for sea ice and an initial guess of the sea ice thickness is first input into the RT-DMPACT forward model. The forward model will then generate a set of radar backscatter data based on the input. SA will then be applied to optimize the difference between the generated radar backscatter data and the measured radar backscatter data by adjusting the sea ice thickness. When the model has achieved global minimum or when the termination criteria is reached, the inverse model stops, and the sea ice thickness that achieves the global minimum is returned as the predicted sea ice thickness. In the next subsection, the RT-DMPACT forward model used will be discussed.

2.1. RT-DMPACT Forward Model

In this study, the sea ice is treated as an electrically dense media [12]. The forward model used in the RTISM-SA to calculate the scattering properties of the sea ice is the RT-DMPACT Forward Model. This forward model uses the Radiative Transfer (RT) theory incorporated with the Dense Medium Phase and Amplitude Correction Theory (DMPACT) [13]. The configuration for the forward model is shown in Figure 2. In this study, the forward model caters for single layer only, where θ and θ_S are defined as the angle of propagation of the incident and scattered wave, respectively.
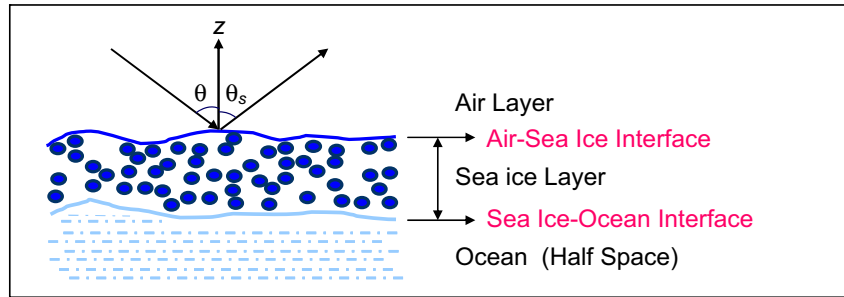

Figure 2. Model configuration for the RT-DMPACT single layer forward model.

From [14–16], the classical formulation of the Radiative Transfer theory used to calculate the propagation and scattering of microwave of a specific intensity in a particular medium is given by:

$$\cos\theta \frac{\partial I}{\partial z} = -\bar{\bar{\kappa}}_e \bar{I} + \int \bar{\bar{P}} \bar{I} \partial\Omega \tag{1}$$

where I, k_e, P, $d\Omega$, and z are the Stokes vector, extinction matrix, phase matrix of the medium, solid angle, and vertical direction, respectively. The scattering and absorption loss of the Stokes vector along a propagation direction has been taken into account by the extinction matrix. The phase matrix, P, from Equation (1) has the following expression:

$$\bar{\bar{P}}\left(\theta,\phi;\theta',\phi'\right) = \left\langle |\psi|^2 \right\rangle_n \cdot \bar{\bar{S}} = \left[\begin{array}{cc} P_{vv} & P_{vh} \\ P_{hv} & P_{hh} \end{array} \right] \tag{2}$$

where $\left\langle |\psi|^2 \right\rangle_n$ is the dense medium phase correction factor, and S is the Stokes matrix for Mie scatterers with Close Spacing Amplitude Correction that relates the scattered intensities to the incident intensities of the scatterer [17].

As the sea ice is treated as an electrically dense medium, the dense medium phase correction factor, $\left\langle |\psi|^2 \right\rangle_n$ from Equation (2), is incorporated into the phase matrix to take into account the coherent

effect of scattering among the scatterers, thus giving a more accurate result. This factor can be further expressed as:

$$\langle |\Psi|^2 \rangle_n = \frac{1 - e^{-k_{si}^2 \sigma^2}}{d^3} + \frac{e^{-k_{si}^2 \sigma^2}}{d^3} \sum_{q=1}^{\infty} \frac{(k_{si}^2 \sigma^2)^q}{q!} \cdot \left[\left(\sqrt{\frac{\pi}{q}} \left(\frac{l}{d} \right) \right)^3 \exp \left(\frac{-k_{si}^2 l^2}{4q} \right) - a\left(k_x\right) a\left(k_y\right) a\left(k_z\right) \right] \quad (3)$$

where σ^2 represents the variance of the positions of the scatterers, k the propagation vector, d the average distance between scatterers, l the correlation length, and $a(k_r)$ is given by:

$$a\left(k_r\right) = \sqrt{\frac{\pi}{q}} \left(\frac{l}{d} \right) \exp \left(\frac{-k_r^2 l^2}{4q} \right) \mathrm{Re} \left\{ erf \left(\frac{(qd/l) + jk_r l}{2\sqrt{q}} \right) \right\} \quad (4)$$

where $erf()$ is an error function that provides approximation for some of the terms in the non-coherent component of the phase correction factor. The detailed formulation and analysis of the DMPACT can be found in [13, 17, 18].

During implementation, the Radiative Transfer equation is first converted into an integral equation, where the equation is then solved iteratively by including boundary conditions. The detailed derivation for solving the Radiative Transfer equation can be found in [19, 20]. The Integral Equation Method (IEM) is then applied to calculate the backscattering effects between the air-sea ice interface and sea ice-ocean interface. A detailed formulation of the above method is given by [21]. The detailed iterative solution of a backscatter model integrating the Radiative Transfer equation, DMPACT and IEM can be found in [22]. The RT-DMPACT forward model is capable of calculating the radar backscatter data for all co- and cross-polarizations (σ_{HH}, σ_{HV}, σ_{VH}, σ_{VV}) from a set of input parameters.

The next subsection will provide a closer look at Simulated Annealing, which is the optimizer for the RTISM-SA.

2.2. Simulated Annealing

Simulated Annealing (SA) is a global optimizer that potentially improves the convergence [11]. It explores the target function's entire space before trying to optimize the function. Doing so allows the algorithm to escape from local optima and locate the global optima. Additionally, the SA has less stringent assumptions, which provides it with the capability to solve functions with ridges and plateaus. Another reason that the authors find SA appealing as the choice of the optimizer is that unlike the LMA, it does not require the calculation of the Jacobian matrices of the problem function with respect to the optimized parameter. This means that should the target parameter change, there is no need to recalculate the Jacobian matrices. This advantage allows the model to become more generalized and makes extension of the model to include retrieval of other parameters possible.

SA is an optimizer designed based on the concept of thermodynamics. SA mimics the process of annealing in metallurgy. Annealing is a technique to heat and cool a molten metal in a controlled manner so that the metal is able to arrive at a low energy state. Inherent random fluctuations in the energy allow the metal to escape the local energy minima to achieve the global minimum, which greatly reduces the metal's defects. However, if the molten metal is cooled without control (quenching), the metal may contain more energy and thus contains more defects. More information about SA can be found in [11].

The SA algorithm implemented in the RTISM-SA is based on the algorithm proposed by Goffe et al. [23]. Goffe et al. made their own modifications to the algorithm initially proposed by Corana et al. [24]. In [23], the following parameters are defined: T_0, the initial temperature; X, the starting vector of parameters; and V, the step length for X. These parameters are essential to maximize any function, $f(X)$. Both X and V are vectors of length n, the number of parameters of the model. The upper case refers to vectors and the lower case to scalars (with the exception of temperature, T). The following summarizes the steps of the algorithm:

1. Function is evaluated at a starting point X, and the value f is obtained.
2. A new X, X' is chosen by varying element i of X: $x_i' = x_i + r \cdot v_i$, where r is a uniformly distributed random number from $[-1, 1]$, and v_i is element i of V.
3. Function value f' is computed.

4. If $f' > f$, X' is accepted and set as X; algorithm moves uphill.

5. If f' is the largest, both f' and X' are recorded as this is the best current optimum.

6. If $f' \leq f$, Metropolis criterion decides acceptance through the application of thermodynamics. The value p is computed: $p = e^{(f'-f)/T}$, and compared with p', a uniformly distributed random number from $[0, 1]$.

7. If $p > p'$, X is accepted as X'; algorithm moves downhill.

8. If $p \leq p'$, X' is rejected. It should be noted that lower temperatures and larger differences in the function's value decrease the probability of a downhill move.

9. After N_S steps through all elements of X, the step length vector V is adjusted so that 50% of all moves are accepted, allowing wider sampling of the function. For example, the relevant element of V is enlarged when a great percentage of points are accepted for x_i. This increases the number of rejections and decreases the percentage of acceptances for a given temperature.

10. After N_T times of steps 1–9, the temperature, T, is reduced: $T' = r_T \cdot T$, where r_T is between 0 and 1; steps 1–9 are repeated again until the conditions in steps 11 and 12 are met.

11. Any downhill move is less probable at a lower temperature, thus increasing the number of rejections and reducing the step lengths. The first point tried at the new T is the current optimum. These two factors allow the algorithm to focus on the most promising area.

12. The last N_ε values of the largest function values from the end of each temperature reduction are compared with the most recent one and the optimum function value. If all differences are less than ε, the algorithm ends, ensuring that global maximum is reached.

As a summary, SA first takes time to explore the surface of the function by moving with large step lengths. As the temperature falls, and the step length is reduced, it begins to focus on the most promising area, while escaping the local maxima through downhill moves. After several iterations, the algorithm then converges to the function's global maximum. In the next section, the methodology to test the RTISM-SA shall be presented.

3. METHODOLOGY

In this study, the RTISM-SA is used to estimate sea ice thickness (parameter X) from radar backscatter data. In the simulations, the radar backscatter data used are either in HH polarization (σ_{HH}), VV polarization (σ_{VV}), or both. The problem function to perform the optimization is given as:

$$f(X)_1 = \varepsilon_\sigma = \sigma'_{HH} - \sigma_{HH} \tag{5}$$

$$f(X)_2 = \varepsilon_\sigma = \sigma'_{VV} - \sigma_{VV} \tag{6}$$

$$f(X)_3 = \varepsilon_\sigma = \left| \left(\sigma'_{VV} - \sigma_{VV}\right)^2 + \left(\sigma'_{HH} - \sigma_{HH}\right)^2 \right| \tag{7}$$

where ε_σ is the error difference, and σ'_{HH} and σ'_{VV} are the estimated radar backscatter data from the RT-DMPACT forward model (by varying parameter X) while σ_{HH} and σ_{VV} are the measured radar backscatter data (using either SAR or scatterometers). The algorithm terminates when the global minimum of ε_σ is found, and X at that point will be the predicted sea ice thickness. For all simulations, two sets of input values are required to set up the RTISM-SA. The first set of input values is to configure the SA while the second set of input values is to set up the RT-DMPACT forward model. For the simulations presented in this paper, the input parameters of the SA are fixed. These values are listed in Table 1. A total of two tests are performed using the RTISM-SA.

For the first test, a theoretical analysis of the RTISM-SA is conducted by setting σ_{HH} as the simulated output from the RT-DMPACT forward model. Before the inversion, a number of testing radar backscatter data are first simulated from the RT-DMPACT model using ground truth measurement data with random selection of sea ice thickness (0.1–2.0 m) and frequencies (1–5 GHz). This set of testing radar backscatter data is then used for the inversion of sea ice thickness to test if the inversion model functions as designed. Table 2 shows the input data into the RT-DMPACT forward model to first obtain the testing radar backscatter data. The same input will then be used during the retrieval as well except for the sea ice thickness which will be estimated by the inversion process.

Table 1. Input parameters for SA for theoretical analysis.

Parameter	Value
Temperature reduction factor, r_T	0.85*
Error tolerance for termination, ε	1.0E-6
Number of cycles, N_S	20*
Number of iterations before temperature reduction, N_T	20
Maximum number of function evaluations	100000
Initial temperature, T_0	5.0
Step length vector, V	1.0*
Vector that controls step length adjustment, C	2.0*
Lower bound for solution variable, L_B	0.1 m
Upper bound for solution variable, U_B	2.0 m
Starting value for variables to be optimized, X	0.1 m $\sim$ 2.0 m

*As recommended in [23].

Table 2. Input parameters for RT-DMPACT forward model for theoretical analysis.

Parameter	Value	
Operating Frequency (GHz)	1 $\sim$ 5	
Incidence Angle (°)	25	
Volume Fraction of Sea Ice	Measured Values	
Scatterer Radius (mm)	Measured Values	
Sea Ice Thickness (m)	0.1 $\sim$ 2.0	
Top Layer Dielectric Constant (Air)	1.0	0.0
Scatterer Permittivity (Brine)	Measured Values	
Background Layer Dielectric Constant (Pure Ice)	3.15*	2.0E-3*
Bottom Layer Dielectric Constant (Ocean)	Measured Values	
Top Surface RMS Height and Correlation Length (m)	Measured Values	
Bottom Surface RMS Height and Correlation Length (m)	2.8E-4**	2.1E-2**

* Values based on [20].
** Values based on [19].

Once the applicability of the RTISM-SA is confirmed, the next step is to assess the function of the RTISM-SA under actual conditions. In this test, the RTISM-SA is used to retrieve sea ice thickness using ground truth measurement data together with actual radar backscatter data extracted from satellite images. Under actual conditions, the retrieval of sea ice thickness becomes complicated as radar backscatter data measured by satellites are subject to actual conditions on the ground due to ever changing weather conditions during satellite image acquisition. In this paper, the work done using measurements carried out in 2006 by the first author is presented. For this test, only single polarization radar backscatter data (σ_{HH}) are used as during 2006, only one Radarsat-1 satellite image was acquired. Additionally, the simulation discussed in this paper will focus only on first year sea ice, where the lack of snow cover allows the conditions of the sea ice to match the inverse model's single layer configuration.

In order to further test the RTISM-SA, the inverse model is then used to retrieve saline ice thickness from the measured data of lab grown saline ice experiments (CRRELEX'93) conducted within a refrigerated facility at the U.S. Army Cold Regions Research and Engineering Laboratory

(CRREL) in 1993. During the experiment, the various physical parameters of lab grown saline ice were measured at fixed intervals. Additionally, a C-band polarimetric scatterometer was also used to obtain the polarimetric signatures of the thin saline ice at different angles during the measurements. Details of the experiment setup, measurement procedures, and measured parameters can be found in Nghiem et al. [25].

For this third test, the RT-DMPACT forward model is first applied to understand the trend of the radar backscatter using different sets of parameters measured at different time intervals as reported in [25]. The difference between this study and the work done in [9, 10] is that due to the absence of the growth model, the retrieval is done separately using parameters measured for each time interval. Another important note is that the current RTISM only caters for spherical scatterers, while the shape of the brine reported in [25] is mainly ellipsoidal. Since the radius of scatterers is an important input for the RTISM, the radius of scatterers for spherical shapes is estimated based on the calculated volume of scatterers for ellipsoidal shapes from measurements reported in [25]. Tables 3 and 4 show the list of input parameters used for the second test. In the next section, the findings and results will be presented.

Table 3. Input parameters for SA for saline ice thickness retrieval.

Parameter	Value
Temperature reduction factor, r_T	0.85*
Error tolerance for termination, ε	1.0E-6
Number of cycles, N_S	20*
Number of iterations before temperature reduction, N_T	20
Maximum number of function evaluations	50000
Initial temperature, T_0	5.0
Step length vector, V	1.0*
Vector that controls step length adjustment, C	2.0*
Lower bound for solution variable, L_B	1 cm
Upper bound for solution variable, U_B	12 cm
Starting value for variables to be optimized, X	1 cm $\sim$ 12 cm

*As recommended in [23].

4. RESULTS

This section presents the results from the two tests discussed in the earlier section. Firstly, the results obtained from the theoretical analysis of the RTISM-SA are discussed. This theoretical analysis is performed to verify the functioning of the RTISM-SA using simulated radar backscatter data. Next, the retrieval of sea ice thickness using ground truth measurement data and Radarsat-1 satellite image data from the year 2006 is presented. Then, the performance of the RTISM-SA used to retrieve saline ice thickness using measurement data obtained from CRRELEX'93 is discussed.

4.1. Theoretical Analysis of RTISM-SA

In this analysis, radar backscatter data are first simulated using the RT-DMPACT forward model for different sets of input parameters randomly chosen within the range of ground truth measurement data collected from Ross Island, Antarctica between the years 2005 and 2008 or estimated based on [19]. Figure 3 shows 15 selected results from the theoretical analysis of the inverse model. In the graph, the estimated sea ice thickness using the RTISM-SA is compared with the randomly chosen sea ice thickness input into the RT-DMPACT. The graph demonstrates that for different sets of input values, the RTISM-SA is capable of determining the sea ice thickness (parameter X) from different starting

Table 4. Input parameters for RT-DMPACT forward model for saline ice thickness retrieval.

Parameter	Value	
Operating Frequency (GHz)	5	
Incidence Angle (°)	25 and 30	
Volume Fraction of Sea Ice	Calculated from [25]	
Scatterer Radius (mm)	Estimated from [25]*	
Saline Ice Thickness (cm)	Estimated from [25]	
Top Layer Dielectric Constant (Air)	1.0	0.0
Scatterer Permittivity (Brine)	Calculated from [25]	
Background Layer Dielectric Constant (Pure Ice)	3.15**	2.0E-3**
Bottom Layer Dielectric Constant (Ocean)	Calculated from [25]	
Top Surface RMS Height and Correlation Length (m)	Estimated from [25]	
Bottom Surface RMS Height and Correlation Length (m)	Estimated from [25]	

* The scatterer radius here is for spherical shape and is estimated from the paper, where the reported scatterer shape is ellipsoidal.

** Values based on [20].

values, giving a good match to the original sea ice thickness, provided the output radar backscatter data from the RT-DMPACT is close to the measured one. Figure 4 demonstrates how the RTISM-SA randomly moves between guesses until it slowly settles on a solution.

Generally, most of the test cases show that the output from the RTISM-SA is able to match the required value. However, special mention needs to be given to test cases 12 and 15 as there is a difference between the predicted sea ice thickness and the actual value, where the sea ice thicknesses are more than 1.5 m. For case 12, simulation was performed at 4 GHz, and the radar backscatter data began to saturate when the sea ice thickness input is more than 1.4 m. For case 15, the frequency was set at 5 GHz, and saturation was observed after the thickness of 1.0 m. Under these circumstances, the variations in the radar backscatter data as the sea ice thickness increases become small. Thus, although the RTISM-SA is able to converge and estimate through the simulation, it is unable to accurately predict the sea ice thickness due to the insensitivity of the forward model when saturation occurs. The next subsection will present the results of sea ice thickness retrieval using single polarization radar backscatter data from Radarsat-1 and ground truth measurement data performed in Ross Island, Antarctica in the year 2006.
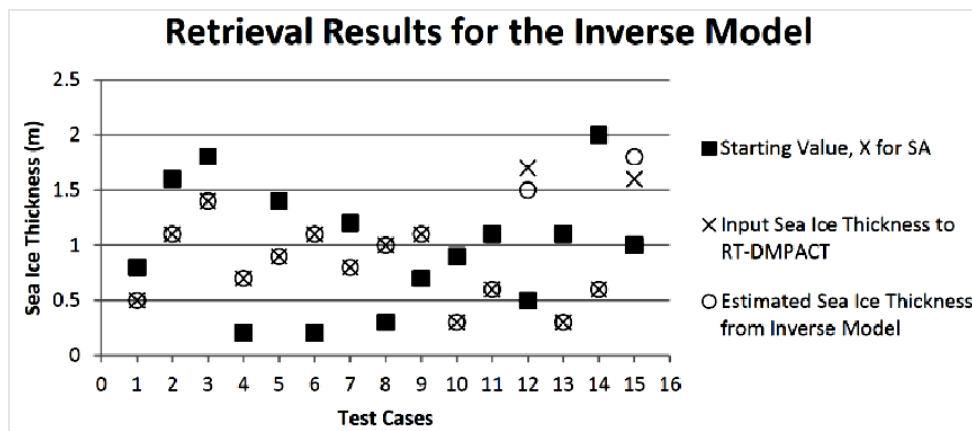
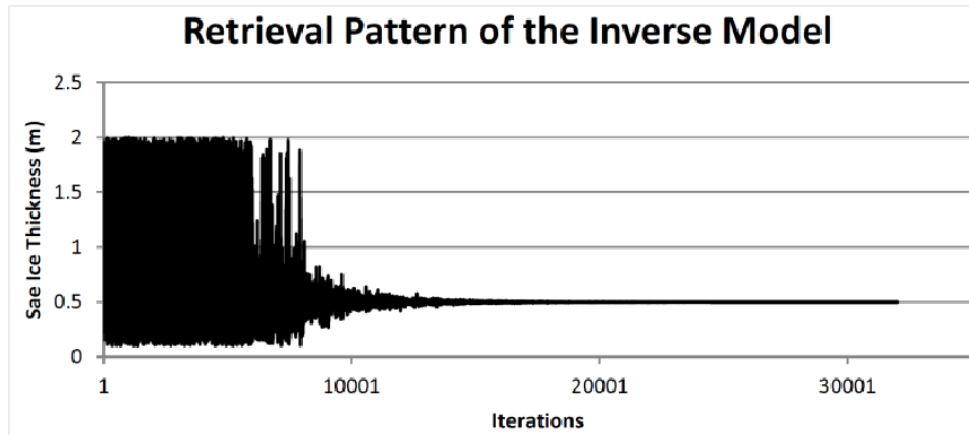**Figure 3.** Theoretical analysis of the RTISM-SA.

Figure 4. Retrieval pattern of the RTISM-SA.

4.2. Sea Ice Thickness Retrieval Using Radarsat-1

In this section, the results of the inverse model to retrieve sea ice thickness using ground truth measurement data and radar backscatter data extracted from Radarsat-1 satellite image for the year 2006 are presented. The Radarsat-1 satellite image was acquired during the ground truth measurement trip carried out by the first author from 19 to 27 October, 2006. The data collected from two of the sites during the trip are used for the retrieval. These sites are located at Cape Evans (166°23.882'E; 77°38.229'S) and Cape Royds (166°11.797'E; 77°33.568'S) in the area of Ross Island, Antarctica, respectively, and the sea ice formed here is the first year sea ice. The lack of snow cover during the time of the ground truth measurement also means that these two sites better matche the model configuration of the RT-DMPACT forward model used in the RTISM-SA. During simulations, the operating frequency and incidence angle are set to 5.3 GHz and 25°, respectively, as these are the specifications given by Radarsat-1.

Table 5 shows the retrieval of sea ice thickness from sites 7 and 9. It is observed that the RTISM-SA is able to provide a prediction for both cases. However, there is some difference between the inversion output and the actual measured sea ice thickness. A sensitivity analysis on the RT-DMPACT forward model using the respective ground truth measurement data from sites 7 and 9 shows that the saturation of radar backscatter data occurred for site 7 after 1.1 m while for site 9 it happened after 0.6 m. The measured sea ice thicknesses at sites 7 and 9 are 1.68 m and 1.60 m, respectively, which shows that the inversion through RTISM-SA operates in the region where the radar backscatter data have saturated with increasing sea ice thickness. This affects the accuracy of the RTISM-SA, though it still predicts the value of sea ice thickness near the actual measured values for the case of site 7, considering that the sea ice thickness in that region can be as thick as 2.3 m from the ground truth measurement. Additionally, for this simulation, only HH polarization radar backscatter data are used for the simulations as only Radarsat-1 satellite image was acquired that year. The lack of multi-polarization data to offset any bias between the simulated and measured radar backscatter data may also be a key factor contributing to the discrepancies between the model predictions and actual measurements of the sea ice thickness. The next subsection will discuss the results of saline ice thickness retrieval using measurement data from CRRELEX'93.

Table 5. Sea ice thickness retrieval for ground truth measurement sites 7 and 9 for year 2006.

Sites	Model Prediction	Measured (m)
Site 7	2.0	1.68
Site 9	0.9	1.60

4.3. Thin Saline Ice Thickness Retrieval

In order to further validate the RTISM-SA, a third test is performed. In this analysis, the results of the saline ice thickness retrieval using RTISM-SA from measured parameters reported in [25] are presented. The first part of this analysis is to use the RT-DMPACT to observe the sensitivity of the radar backscatter data as the saline ice thickness increases. The simulation uses parameters measured in [25] at various time intervals during different growth stages of the saline ice as input for the forward model. For this analysis, only co-polarization data are used.

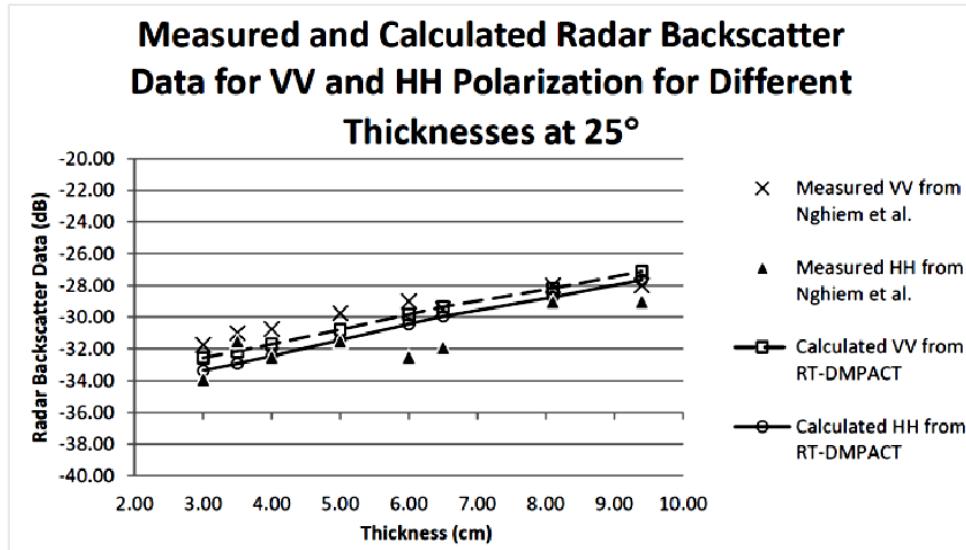Figures 5 and 6 show a summary of the measured and calculated radar backscatter data for VV and

Figure 5. Summary of measured and calculated radar backscatter data simulated using the RT-DMPACT forward model for VV and HH polarization at 25°.
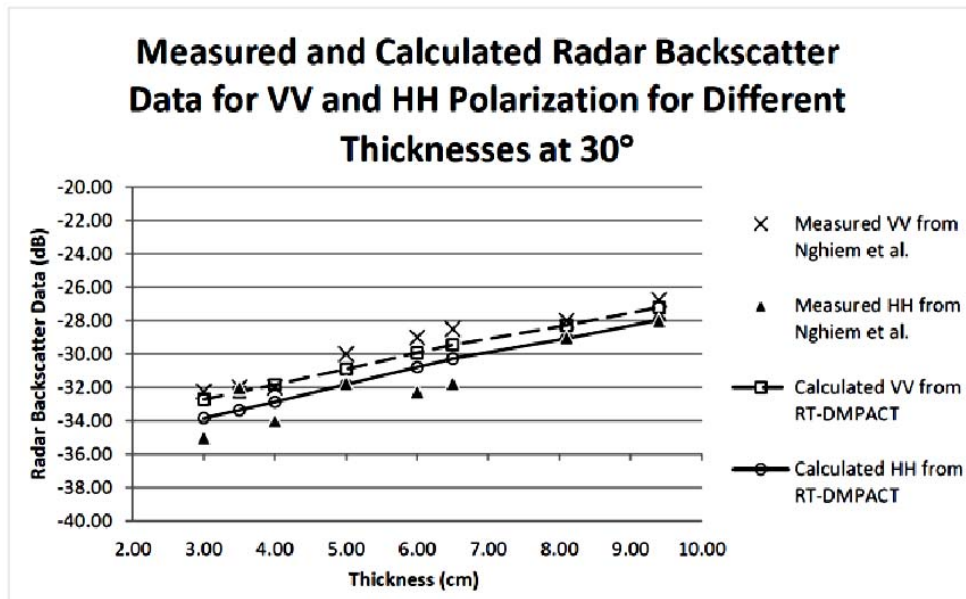

Figure 6. Summary of measured and calculated radar backscatter data simulated using the RT-DMPACT forward model for VV and HH polarization at 30°.

HH polarizations at specific saline ice thicknesses for incidence angles of 25° and 30°, respectively. Due to the lack of measurement data for some of the parameters after the saline ice thickness of 9.4 cm [25], the comparison will cover only from 3 cm to 9.4 cm. From the figures, it is observed that there are similar trends for VV and HH polarizations between the simulated output from RT-DMPACT and the measurements from [25]. However, it is also observed that there are differences between the simulated output and the measured data for each polarization, which may lead to errors during the retrieval process. One of the possible solutions to reduce the effects which these errors may have on the retrieval results is to extend the RTISM-SA to include multi-polarization data. While not all cases may yield results free of error, it at least helps to reduce the error to within an acceptable margin.

The retrieval of the saline ice thickness is performed first using single polarization data followed by multi-polarization data for both VV and HH polarizations. The results of the retrieval are presented in Figure 7 for incidence angles 25° and 30°. Results show that the RTISM-SA performs as expected, but the success and accuracy of the prediction rely on the accuracy of the forward model. For single polarization VV, for both incidence angles, the retrieved thickness tends to have a bias higher than the measured values while for single polarization HH, the reverse holds true. This is probably due to the differences between the RT-DMPACT forward model simulations and the measured radar backscatter reported in [25], which can be observed from Figures 5 and 6.
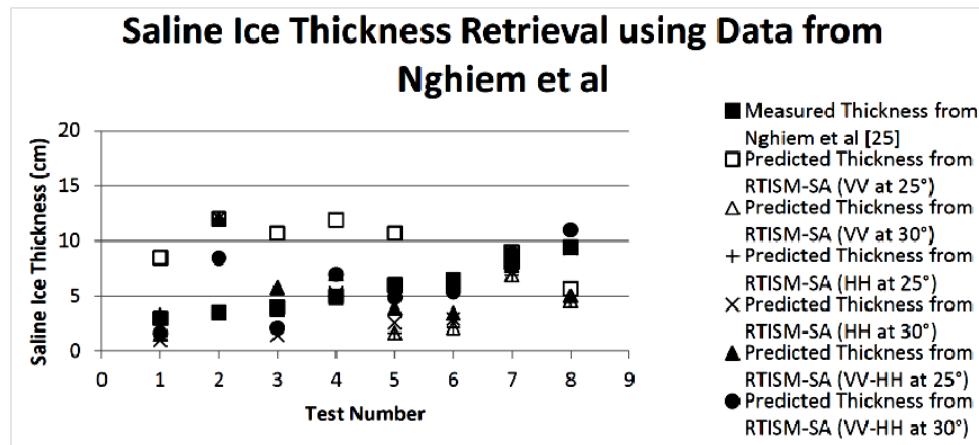

Figure 7. Retrieval results for saline ice thickness using RTISM-SA and data from Nghiem et al. [25].

The retrieval results using multi-polarization data appear to give a better agreement than that using single polarization data. Except for test number 2 (which corresponds to saline ice thickness of 3.5 cm), most of the test numbers show good comparison between the predicted and measured thicknesses, as shown in Figure 7. The reason for this is that for the set of parameters at 3.5 cm obtained from [25], the simulated output from the RT-DMPACT forward model is always lower for VV and HH polarizations for both incidence angles than the measured radar backscatter from [25]. As such, the prediction will tend to approach the upper limit set for the SA, thus resulting in a less accurate prediction. Lastly, from the simulations, it also appears that the results from the incidence angle 30° are slightly better than 25°.

5. CONCLUSION AND FUTURE WORK

In this study, an inverse model for sea ice thickness retrieval, RTISM-SA, is presented. The use of SA as the optimizer in the RTISM-SA has given the model better adaptability and the potential to extend to retrieval of other parameters than thickness in the future. The theoretical analysis of the model under ideal conditions where the RT-DMPACT forward model matches the measured values has proved that the model is working as expected and has the potential to predict sea ice thickness from radar backscatter data. The next test is to try the retrieval of sea ice thickness using the RTISM-SA

under actual conditions. The retrieval of sea ice thickness using ground truth measurement data from Ross Island, Antarctica and radar backscatter data from Radarsat-1 during 2006 shows the potential of the inverse model. As Radarsat-1 only measures HH polarization radar backscatter data, the results show that the inverse model is capable of converging and giving a result, but the accuracy is not that good. A third test utilizing measured data from CRRELEX'93 reported in [25] is performed to better validate the performance of the RTISM-SA. The test, which only utilized HH and VV polarization radar backscatter data, shows that the RTISM-SA's performance relies on the accuracy of the forward model, but with the use of multi-polarization data, the errors in the retrieval of saline ice thickness can be reduced to reach a better agreement with the measured results. In the future, improvements to the RT-DMPACT forward model can be considered to allow the RTISM-SA to give better predictions. Suggested improvements here are to include multiple surface scattering calculations for better cross-polarization radar backscatter data calculations and modification of the model configuration to include ellipsoidal shaped scatterers. Next, a comprehensive study into how the various input parameters of the SA affect the retrieval results might provide better options on how to set up the SA for future simulations.

ACKNOWLEDGMENT

REFERENCES

1. Turner, J. and J. Overland, "Contrasting climate change in the two polar regions," *Polar Research*, Vol. 28, 146–164, 2009.

2. Rack, W. and H. Rott, "Further retreat of the northern Larsen Ice Shelf and collapse of Larsen B," *FRISP Report*, No. 14, 2002.

3. Martin-Mikle, C. J. and D. B. Fagre, "Glacier recession since the Little Ice Age: Implications for water storages in a Rocky Mountain landscape," *Arctic, Antarctic, and Alpine Research*, Vol. 51, No. 1, 280–289, 2019.

4. Stroeve, J. and D. Notz, "Changing state of Arctic sea ice across all seasons," *Environmental Research Letters*, Vol. 13, No. 10, 1–23, 2018.

5. Maykut, G. A., "Energy exchange over young sea ice in the central Arctic," *Journal of Geophysical Research*, Vol. 83, No. C7, 3646–3658, 1978.

6. Golden, K. M., M. Cheney, K. H. Ding, A. K. Fung, T. C. Grenfell, D. Isaacson, J. A. Kong, S. V. Nghiem, J. Sylvester, and D. P. Winebrenner, "Forward electromagnetic scattering models for sea ice," *IEEE Transactions on Geoscience and Remote Sensing*, Vol. 36, No. 5, 1655–1674, 1998.

7. Golden, K. M., D. Borup, M. Cheney, E. Cherkaeva, M. S. Dawson, K. H. Ding, A. K. Fung, D. Isaacson, S. A. Johnson, A. K. Jordan, J. A. Kong, R. Kwok, S. V. Nghiem, R. G. Onstott, J. Sylvester, D. P. Winebrenner, and I. H. H. Zabel, "Inverse electromagnetic scattering models for sea ice," *IEEE Transactions on Geoscience and Remote Sensing*, Vol. 36, No. 5, 1675–1704, 1998.

8. Lee, Y. J., W. K. Lim, and H.-T. Ewe, "A study of an inversion model for sea ice thickness retrieval in Ross Island, Antarctica," *Progress In Electromagnetics Research*, Vol. 111, 381–406, 2011.

9. Shih, S. E., K. H. Ding, S. V. Nghiem, C. C. Hsu, J. A. Kong, and A. K. Jordan, "Thickness retrieval using time series electromagnetic measurements of laboratory grown saline ice," *1996 International Geoscience and Remote Sensing Symposium (IGARSS'96), Vol. 2: Remote Sensing for a Sustainable Future*, 1208–1210, 1996.

10. Shih, S. E., K. H. Ding, S. V. Nghiem, C. C. Hsu, J. A. Kong, and A. K. Jordan, "Saline ice thickness retrieval using time series c-band polarimetric radar measurements," *IEEE Transactions on Geoscience and Remote Sensing*, Vol. 36, No. 5, 1589–1598, 1998.

11. Press, W. H., S. A. Teukolsky, W. T. Vetterling, and B. P. Flannery, *Numerical Recipes: The Art of Scientific Computing*, Cambridge University Press, New York, 1986.

12. Albert, M. D., T. E. Tan, H. T. Ewe, and H. T. Chuah, "A theoretical and measurement study of sea ice and ice shelf in Antarctica as electrically dense media," *Journal of Electromagnetic Waves and Applications*, Vol. 19, No. 14, 1973–1981, 2005.

13. Chuah, H. T., S. Tjuatja, A. K. Fung, and J. W. Bredow, "A phase matrix for a dense discrete random medium: Evaluation of volume scattering coefficient," *IEEE Transactions on Geoscience and Remote Sensing*, Vol. 34, No. 5, 1137–1143, 1996.

14. Chandrasekhar, S., *Radiative Transfer*, Dover, New York, 1960.

15. Ulaby, F. T., R. K. Moore, and A. K. Fung, *Microwave Remote Sensing, Active and Passive: Vol. 1. Microwave Remote Sensing Fundamentals and Radiometry*, Addison-Wesley Publishing Company, Massachusetts, 1981.

16. Tsang, L., J. A. Kong, and R. T. Shin, *Theory of Microwave Remote Sensing*, Wiley-Interscience, New York, 1985.

17. Fung, A. K. and H. J. Eom, "A study of backscattering and emission from closely packed inhomogeneous media," *IEEE Transactions on Geoscience and Remote Sensing*, Vol. 23, No. 5, 761–767, 1985.

18. Ewe, H. T. and H. T. Chuah, "An analysis of the scattering of discrete scatterers in an electrically dense medium," *1998 IEEE International Geoscience and Remote Sensing Symposium Proceedings (IGARSS'98)*, Vol. 5, 2378–2380, July 6–10, 1998.

19. Fung, A. K., *Microwave Scattering and Emission Models and Their Applications*, Artech House, Norwood, 1994.

20. Ulaby, F. T., R. K. Moore, and A. K. Fung, *Microwave Remote Sensing, Active and Passive: Vol. 3, From Theory to Applications*, Addison-Wesley Publishing Company, Massachusetts, 1986.

21. Fung, A. K., Z. Li, and K. S. Chen, "Backscattering from a randomly rough dielectric surface," *IEEE Transactions on Geoscience and Remote Sensing*, Vol. 30, No. 2, 356–369, 1992.

22. Ewe, H. T., H. T. Chuah, and A. K. Fung, "A backscatter model for a dense discrete medium: Analysis and numerical results," *Remote Sensing of Environment*, Vol. 65, No. 2, 195–203, 1998.

23. Goffe, W. L., G. D. Ferrier, and J. Rogers, "Global optimization of statistical functions with simulated annealing," *Journal of Econometrics*, Vol. 60, Nos. 1–2, 65–99, 1994.

24. Corana, A., M. Marchesi, C. Martini, and S. Ridella, "Minimizing multimodal functions of continuous variables with the 'simulated annealing algorithm,"' *ACM Transactions on Mathematical Software*, Vol. 13, No. 3, 262–280, 1987.

25. Nghiem, S. V., R. Kwok, S. H. Yueh, A. J. Gow, D. K. Perovich, J. A. Kong, and C. C. Hsu, "Evolution in polarimetric signatures of thin saline ice under constant growth," *Radio Science*, Vol. 32, No. 1, 127–151, 1997.